European Journal of Immunology

WILEY-VCH

European Journal of Immunology
Basic • Clinical • Translational

RESEARCH ARTICLE OPEN ACCESS

Systems Immunology

Single-Cell Profiling of Splenic Immune Ageing and Chronic Stress Adaptations in Mice With Natural Microbiota

Chinna Susan Philip[1] | Igor Filippov[1,2] | Uku Haljasorg[1] | Pärt Peterson[1]

[1]Molecular Pathology Research Group, Institute of Biomedicine and Translational Medicine, University of Tartu, Tartu, Estonia | [2]QIAGEN Aarhus A/S, Aarhus, Denmark

Correspondence: Chinna Susan Philip (chinna.susan.philip@ut.ee)

Received: 1 September 2025 | **Revised:** 26 February 2026 | **Accepted:** 27 February 2026

Keywords: ageing | chronic stress | spleen | T cells | transcriptomic

ABSTRACT

Immune ageing impairs adaptive and innate responses, yet the spleen remains underexplored by cross-cohort single-cell studies. We profiled splenocytes from young, old and chronically stressed old mice with natural microbiota using single-cell RNA sequencing. Ageing was characterised by reduced lymphocyte competence and elevated stress responses. Within *Gzmk*$^{+}$ CD8^{+} T cells, young mice were enriched for Gzmk-high cells, whereas in old mice, both Gzmk-high and Gzmk-low cells showed greater heterogeneity and functional alterations: exhaustion in Gzmk-high and inflammation in Gzmk-low cells. Natural killer (NK) cells and macrophages exhibited reduced cytotoxic potential and sustained pro-inflammatory polarisation, respectively. Chronic stress caused modest compositional shifts that partially counteracted age-related changes. Furthermore, we integrated our dataset with six published datasets to build a comprehensive atlas with > 272,000 splenocytes. Atlas-level annotation showed reproducible compositional shifts across datasets. Conserved ageing signatures included loss of NK effector genes (*Zeb2, Prf1*), decline of naïve T quiescence (*Lef1, Il7r*) with stress induction (*Rbm3, Socs3*), gain of survival/pro-inflammatory/exhaustion genes (*Bcl2, S100a6, Ccl5, Lag3*) in effector T cells, and altered differentiation and regulation (*Zbtb32, Zbtb20, Zfp318, Ighd, Cr2*) in B cells. Our results define conserved features of splenic immunosenescence and provide an atlas for dissecting splenic immune alterations.

1 | Introduction

Ageing causes substantial alterations in immune cell composition, transcriptome, and function across tissues [1, 2]. As primary lymphoid organs involute and reduce immune cell output, the largest secondary lymphoid organ, the spleen, becomes increasingly important [3, 4]. Thymic T cell output declines dramatically with age in humans, emphasising the role of the spleen in peripheral T cell expansion during immune challenges [5, 6]. However, the ageing spleen itself undergoes considerable structural, cellular, and functional changes that disrupt homeostasis and diminish immune responses [3, 7].

Ageing creates an immune imbalance in the lymphoid compartment: naïve T cells decrease while effector T cells increase; transitional (TrB), marginal zone (MZB) and germinal centre (GC B) B cells decline while Apoe-high (Apoe-hi) and age-associated B cells (ABCs) expand; and natural killer (NK) cells reduce [8–12]. Myeloid compartment shows similar age-dependent shifts and dysfunction in monocytes, dendritic cells (DCs), macrophages, neutrophils, and basophils [13–15].

Transcriptional dynamics within and between immune cell types drive this age-associated immune remodelling. Single-cell RNA sequencing (scRNA-seq) studies have defined transcriptional

Abbreviations: ABCs, age-associated B cells; CVS, chronic variable stress; DC, dendritic cell; DEG, differentially expressed gene; EM, effector memory; GC, germinal centre; NK, natural killer; NM, natural microbiota; pDC, plasmacytoid dendritic cell; scRNA-seq, single-cell RNA sequencing; SPF, specific pathogen-free; Tfh, T follicular helper; Treg, regulatory T.

ageing signatures in the spleen, identifying unique age-associated populations such as *Gzmk*$^+$ CD8$^+$ T cells and Apoe-hi B cells [8, 16]. While these findings highlight the complexity of immune ageing, most insights have been derived from specific pathogen-free (SPF) mice, which may not fully recapitulate the impact of commensal microbiota and environmental stressors on immune ageing.

Chronic stress accelerates ageing and alters splenic architecture and cellularity, yet its convergence with intrinsic ageing pathways remains poorly characterised [17–20]. While recent interventions like heterochronic parabiosis and platelet factor exposure show promise in ameliorating immune decline, the baseline transcriptional landscape of the ageing spleen, especially in the context of natural microbiota (NM) and stressors, remains poorly understood [21, 22].

To address these gaps, we performed scRNA-seq on spleens from young, old, and stressed old mice with NM (NM mice), capturing environmental microbial and chronic stress influences on immune ageing. Furthermore, we integrated our data with publicly available SPF datasets, uniformly re-annotating cell types to build a comprehensive ageing murine spleen atlas. This approach validated age-associated compositional changes across datasets and identified robust transcriptional ageing signatures, providing insights into microbiome and chronic stress impacts while offering a foundational resource for studying age-associated immune dysfunction.

2 | Results

2.1 | Study Overview

To examine transcriptomic alterations in the murine splenic immune landscape during ageing, we generated a scRNA-seq dataset comprising splenocytes isolated from young (4-month-old) and old (22–24-month-old) NM mice (Figure 1A). To further investigate the transcriptional impact of chronic stress, we subjected old NM mice to a 14-day chronic variable stress (CVS) regimen (Table S1A). Consistent with systemic stress response, CVS-treated NM mice showed reduced body weight and elevated circulating corticosterone levels compared to age-matched controls (Figure S1A,B).

2.2 | Age-Associated Remodelling of Splenic Immune Landscape

After quality control (QC) and integration, 78,185 splenocytes from young control (young), old control (old), and stressed old (old stressed) NM mice (Figure S1C,D) were annotated into specific cell subsets using canonical markers (Figure 1B,C). Ageing primarily altered lymphoid cells (Figure 1D,E), with significant reductions in certain myeloid cells (macrophages, plasmacytoid dendritic cells [pDCs], and basophils) (Figure 1F) (Figure S2).

Differentially expressed gene (DEG) analysis revealed aged NK cells downregulated genes involved in migration (*Ccr2, Rasgrp2*), maturation (*Eomes, Klra3*) and cytotoxicity (*Prf1, Mndal*) while upregulating survival genes (*Ern1, Atr, Hdac9, Nr3c2*) (Figure 1G) (Table S2). Aged pDCs showed upregulation of inflammation-associated gene *Il31ra* (Table S2). Aged macrophages exhibited a pro-inflammatory but functionally impaired phenotype, characterised by upregulation of inflammatory mediators (*Havcr2, Mefv, Il31ra, Itgax, Nrp2, Nr3c2, P2ry14, Tgfbi*) and loss of interferon response (*Oas2, Mndal, Ddx60, Slfn5, Ifi44, Herc6, Eif2ak2, Il15*) and function-associated genes (*Axl, Siglec1, Hmox1, C2, Hpgd*) (Figure 1G) (Table S2). Both classical and non-classical monocytes shared downregulation of Type I interferon-related genes (*Oas3, Irf7, Ifi44, Ifitm3, Eif2ak2, Oas2, Oasl1*) and upregulation of inflammation-regulating genes (*Cfh, Cd274*) (Figure 1G) (Table S2).

Chronic stress minimally altered splenocyte proportions and transcriptomic profiles (Figure 1D–F) (Table S2). Notably, CVS partially reversed ageing trends by increasing T cells, proliferating B cells and myeloid cells while reducing B cells and proliferating T cells, suggesting compensatory immune remodelling (Figure S3).

2.3 | Age-Induced Alterations in T Cell Heterogeneity and Transcriptional Programmes

To explore the effects of ageing on T cell diversity, we performed high-resolution sub-clustering of T cells and identified naïve CD4$^+$ and CD8$^+$ (CD4N, CD8N), CD4$^+$ and CD8$^+$ effector memory (EM) (CD4EM, CD8EM), CD8$^+$ *Gzmk*$^+$ EM (CD8EM Gzmk+), T helper 2 (Th2) cells, naïve regulatory T (nTregs), effector Tregs (eTregs), non-lymphoid tissue-like Tregs (NLT-like Tregs), T follicular helper (Tfh), $\gamma\delta$ T, and proliferating T cells (Figure 2A,B). Ageing caused a distinct shift from naïve to EM phenotypes with expansion of eTregs and Tfh cells (Figure 2C,D) (Figure S4A). CVS did not alter T cell proportions in stressed old mice (Figure 2C,D) (Figure S4B).

DEG analysis revealed 41 shared ageing DEGs across naïve T cell subsets, including downregulation of quiescence and migration (*Lef1, Tnik*, *Actb, Mtss1, Nedd9*) with shared upregulation of differentiation (*Il2rb, Il18r1, Sgk1, Igf1r*), negative regulators of inflammation (*Tnfaip3, Socs3, Casp, Pros1, Nt5e*) and stress response genes (*Map3k5, Nr3c2*) (Figure 2E) (Tables S3 and S4A). EM subsets showed similar patterns (*Nr3c2, Il18r1* upregulated; *Actb* downregulated) (Figure 2F) (Tables S3 and S4B). Thus, ageing redirects T cells from quiescence towards stress-adapted activation.

2.4 | Transcriptional Heterogeneity of *Gzmk*$^+$ CD8$^+$ T Cells

Gzmk$^+$ CD8$^+$ T cells, previously described as age-associated T cells in SPF mice [16], increased with ageing but showed high interindividual variability in old NM mice (Figure S4A, B). To further understand the dynamics of these cells, we re-clustered CD8EM Gzmk+ cells and annotated them as CD8EM Gzmk-hi and CD8EM Gzmk-lo, based on varying *Gzmk* levels (Figure 3A). The top DEGs indicated CD8EM Gzmk-hi were self-renewing (*Tcf7, Il7r, Bach2, Zeb1*) while CD8EM Gzmk-lo were tissue-resident with effector potential (*Zeb2, Runx1, Il18rap, Cd226*) (Figure S4C).

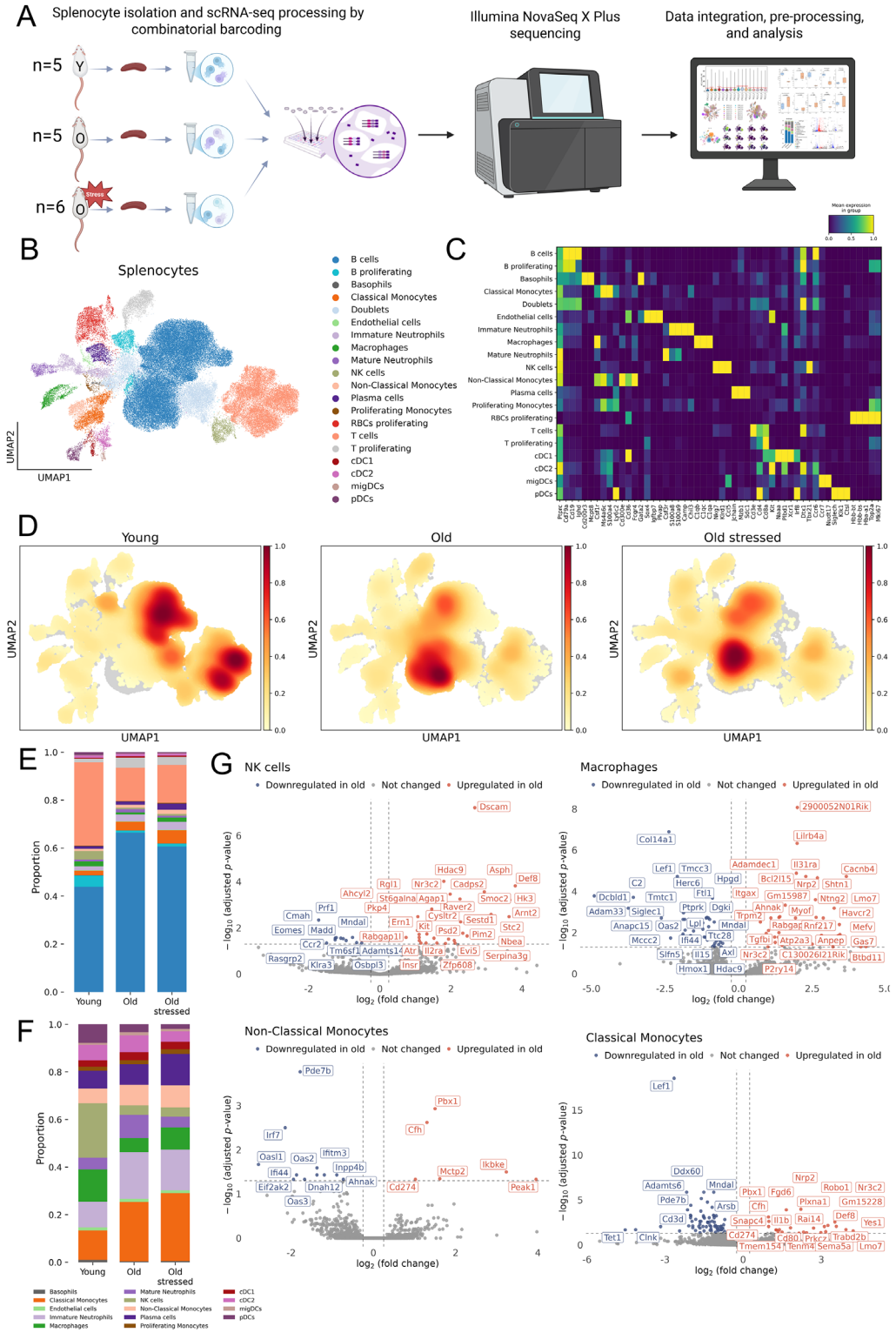

FIGURE 1 | Single-cell immune landscape of splenocytes from young ($n = 5$), old ($n = 5$), and old stressed ($n = 6$) NM mice. (A) Schematic overview of experimental workflow created in BioRender. (B) UMAP representing splenocyte subsets identified by Leiden clustering and marker gene expression including B cells, T cells, NK cells, macrophages, classical and non-classical monocytes, conventional DCs (cDC1, cDC2), migratory DCs (migDCs), plasmacytoid DCs (pDCs), plasma cells, immature and mature neutrophils, basophils, endothelial cells, and proliferating cells. (C) Expression heatmap depicting cell type-specific marker genes. Scale represents mean gene expression per subset. (D) UMAP density plots of splenocyte distributions across groups. (E) Relative proportion of splenocyte subsets across groups. Each stacked bar represents one group normalised to 1.0 indicating 100% of cells within a group and each colour represents one cell type. (F) Relative proportion of splenocyte subsets, excluding T and B cell subsets, across groups. Each stacked bar represents one group normalised to 1.0 indicating 100% of cells within a group and each colour represents one cell type. (G) Volcano plots of DEGs in old versus young mice by cell type. Blue and red dots represent DEGs with mean normalised count < 10 and > 10, respectively. Significant DEGs have adjusted p-value (Benjamini–Hochberg correction) < 0.05 and absolute $\log_2$(fold change) > 0.25.

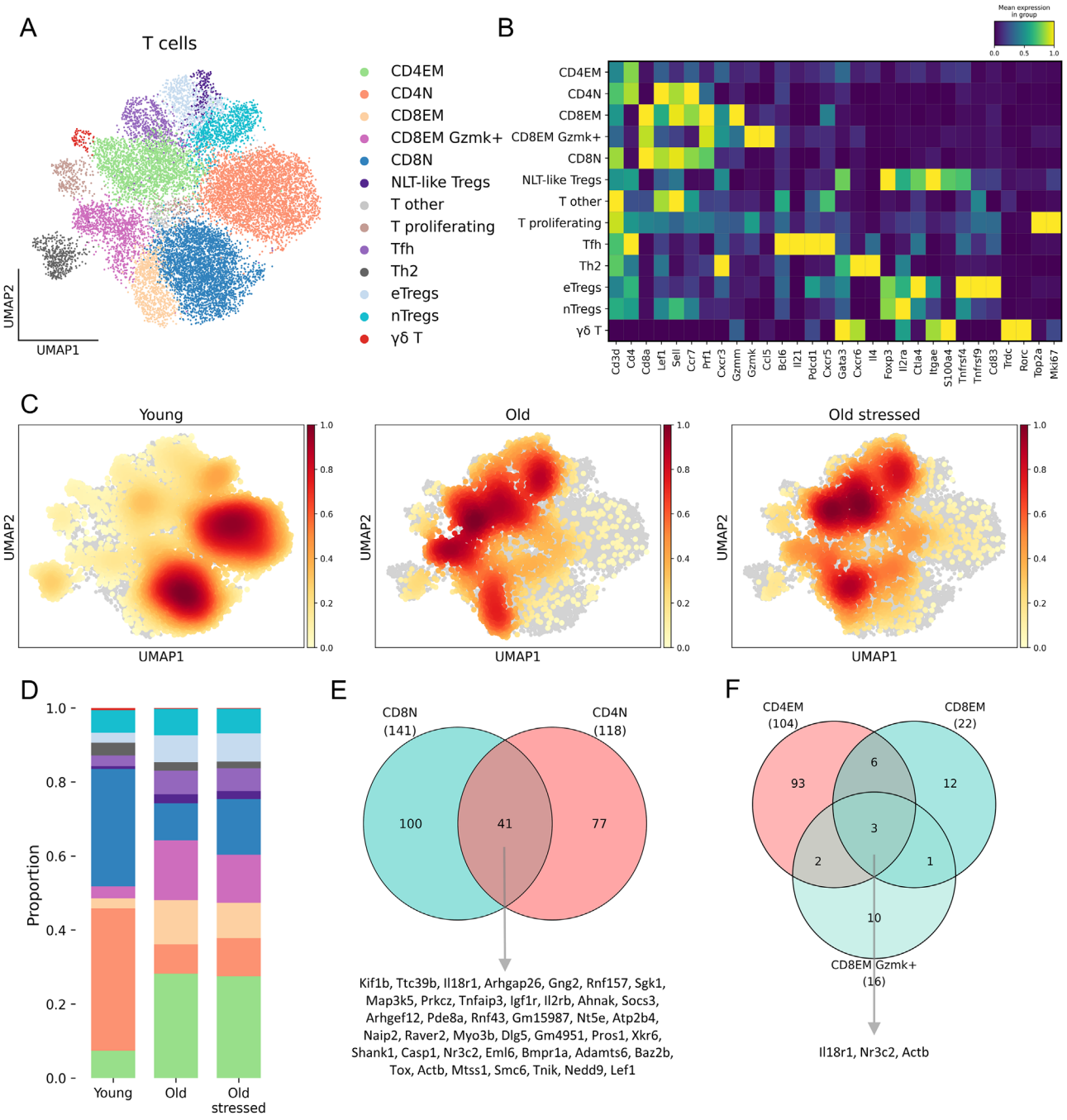

FIGURE 2 | Single-cell transcriptomic profile of splenic T cell subsets from young ($n = 5$), old ($n = 5$), and old stressed ($n = 6$) NM mice. (A) UMAP of T cell subsets identified by Leiden clustering and marker gene expression including naïve (CD4N, CD8N), effector memory (CD4EM, CD8EM), $CD8^+$ $Gzmk^+$ EM (CD8EM Gzmk+), T helper 2 (Th2) cells, naïve regulatory T (nTregs), effector Tregs (eTregs), non-lymphoid tissue-like Tregs (NLT-like Tregs), T follicular helper (Tfh), $\gamma\delta$ T, and proliferating T cells. (B) Expression heatmap of canonical marker genes for T cell subset annotation. (C) UMAP density distributions of T cell subsets across groups. (D) Relative proportion of T cell subsets across groups. Each stacked bar represents one group normalised to 1.0 indicating 100% of cells within a group and each colour represents one cell type. (E) Venn diagram displaying unique and intersecting ageing DEGs among naïve T cell subsets. (F) Venn diagram displaying unique and intersecting ageing DEGs among effector memory T cell subsets. Significant DEGs have adjusted p-value (Benjamini–Hochberg correction) < 0.05 and absolute $\log_2$(fold change) > 0.25.

Ageing shifted proportions to CD8EM Gzmk-lo, which CVS partially mitigated (Figure 3B,C). However, relative proportions of CD8EM Gzmk-hi and -lo remained unchanged with increased heterogeneity in aged mice (Figure 3D). Aged CD8EM Gzmk-hi cells showed loss in migration-related (*Itgb1, Actb, Tmsb4x*) and anti-viral (*Epsti1*) genes with gain of differentiation/exhaustion (*Il18r1, Tigit*) and stress/survival (*Nr3c2, Bcl2*) genes (Figure 3E). Aged CD8EM Gzmk-lo cells showed reduced migration and effector (*Itga4, Ccl5, Epsti1*) genes with increased inflammation (*Il18r1, P2rx7*) genes (Figure 3E). Thus, ageing imposes distinct vulnerabilities on CD8EM Gzmk+ subsets, exhaustion in CD8EM Gzmk-hi and inflammation in CD8EM Gzmk-lo.

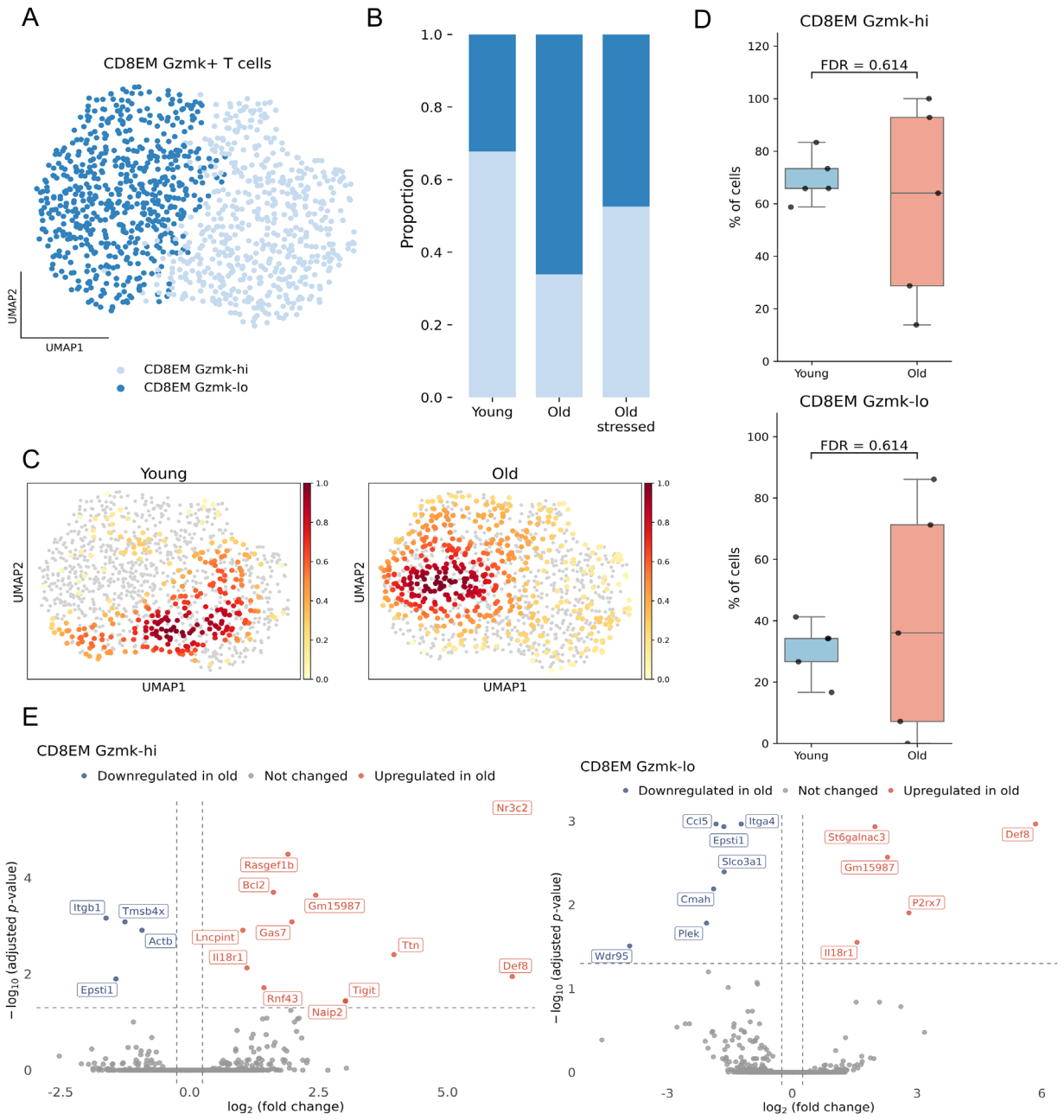

FIGURE 3 | Heterogeneity of splenic *Gzmk*$^+$ CD8$^+$ T cells at single-cell resolution in young ($n = 5$), old ($n = 5$), and old stressed ($n = 6$) NM mice. (A) UMAP representing CD8EM Gzmk+ T cell subsets identified as CD8EM Gzmk-hi and CD8EM Gzmk-lo by Leiden clustering and marker gene expression. (B) Relative proportion of CD8EM Gzmk+ subsets across groups. Each stacked bar represents one group normalised to 1.0 indicating 100% of cells within a group and each colour represents one cell type. (C) UMAP density distributions of T cell subsets across groups. (D) Relative proportions of CD8EM Gzmk+ subsets in young versus old mice. Boxplots display median (centre line), interquartile range (IQR) (box) and whiskers (1.5 × IQR). Dots represent biological replicates. Statistical comparisons were performed using Welch's *t*-test with Benjamini–Hochberg correction (FDR < 0.05). (E) Volcano plots of DEGs in old versus young mice by cell type. Blue and red dots represent DEGs with mean normalised count < 10 and > 10, respectively. Significant DEGs have adjusted *p*-value (Benjamini–Hochberg correction) < 0.05 and absolute $\log_2$(fold change) > 0.25.

2.5 | Age-Associated Changes in Splenic B Cells

To explore the effects of ageing on B cell diversity, B cells were sub-clustered and annotated as TrB, follicular (FoB), GC B, MZB, regulatory (Bregs), memory (memory B), Apoe-hi B, ABCs, and proliferating B cells based on established marker genes (Figure 4A,B). Ageing expanded mature (memory B, Apoe-hi B, and ABCs) and regulatory phenotypes (Bregs) while depleting naïve (TrB, FoB, and MZB) and GC B subsets (Figure 4C,D) (Figure S5A). CVS enhanced TrB depletion and increased Bregs, suggesting enhanced regulatory bias under glucocorticoid exposure (Figure S5B).

In naïve subsets, among the six shared upregulated DEGs, genes associated with migration (*Nrp2*) and stress-response (*Nr3c2*) were identified (Figure 4E) (Table S6A). Mature subsets showed three upregulated genes linked to migration (*Nrp2*) and immunoregulation (*Cd200*), and 11 downregulated genes linked

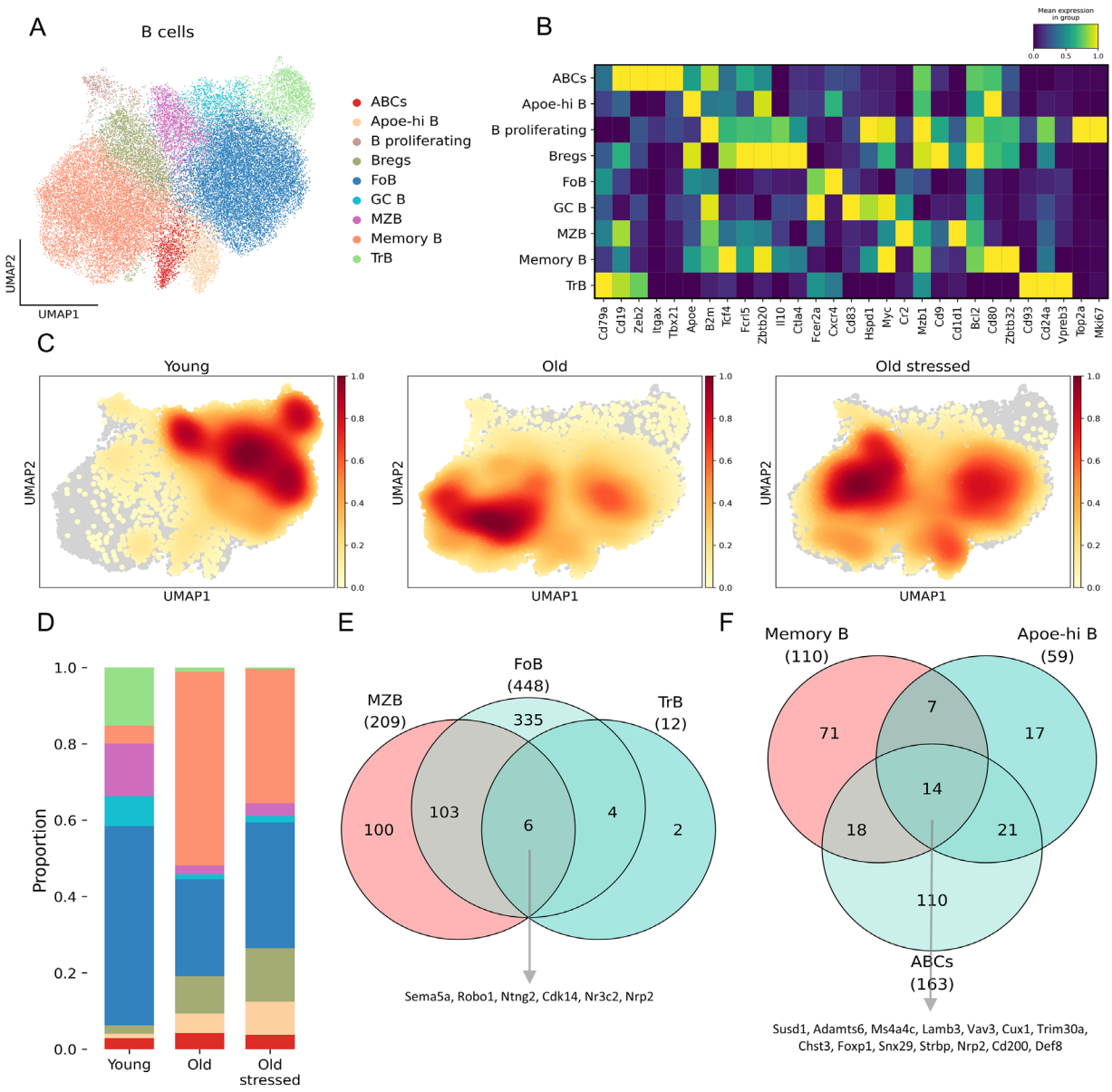

FIGURE 4 | Splenic B cell profile at single-cell resolution from young ($n = 5$), old ($n = 5$), and old stressed ($n = 6$) NM mice. (A) UMAP of B cell subsets identified by Leiden clustering and marker gene expression including transitional (TrB), follicular (FoB), germinal centre (GC B), marginal zone (MZB), regulatory (Bregs), memory (memory B), Apoe-hi B, age-associated (ABCs), and proliferating B cells. (B) Expression heatmap of canonical marker genes for B cell annotation. (C) UMAP density plots showing B cell distributions across conditions. (D) Relative proportion of B cell subsets across groups. Each stacked bar represents one group normalised to 1.0 indicating 100% of cells within a group and each colour represents one cell type. (E) Venn diagram of unique and intersecting ageing DEGs among naïve B cell subsets. (F) Venn diagram of unique and intersecting ageing DEGs among mature B cell subsets. Significant DEGs have adjusted p-value (Benjamini–Hochberg correction) < 0.05 and absolute $\log_2$(fold change) > 0.25.

to differentiation (*Foxp1, Cux1*) and activation (*Vav3, Ms4a4c*) (Figure 4F) (Table S6B). Together, ageing B cells showed dysregulated differentiation and activation but increased migratory and survival capacity.

2.6 | Constructing an Integrated Single-Cell Transcriptomic Atlas of the Ageing Spleen

To generate a comprehensive view of splenic immune ageing, we integrated our NM mice dataset with five published SPF murine scRNA-seq datasets, labelled SPF1–5 [1, 8, 16, 21, 22], creating an atlas of 272,850 splenocytes (Figures S6 and S7). For T cell analysis, we integrated a sixth dataset (SPF6) with re-clustered T cells from the atlas [23]. Dataset-specific details are in Table S1B. NM mice dataset contributed 78,185 cells to the atlas, while SPF1–6 contributed cells ranging from 14,178 to 84,257 (Figure S8A). Three datasets profiled steady-state ageing, whereas others included stress, parabiosis or platelet factor exposure, enabling comparison of canonical and context-specific signatures. Our integrated ageing analysis focused on 203,937 young and old splenocytes (Figure S8B).

Atlas-level annotation identified all major splenic immune lineages, with B cells being most abundant, followed by T cells and resolved populations like exposed macrophages and resident

monocytes not distinguished in NM mice dataset (Figure 5A). Cell type proportions were broadly consistent across datasets except from higher doublets in NM mice (Figure S8C). Thus, we generated a cross-strain, cross-platform resource to detect universal ageing trajectories as well as context-dependent variation.

2.7 | Cross-Dataset Analysis Identifies Conserved Lymphoid Cell Ageing Features

Ageing consistently reduced NK cells and pDCs while increasing immature neutrophils and plasma cells across datasets (Figure 5B) (Figure S9). Young NM mice showed lower proportions of B cells, NK cells, cDC1 and cDC2 with higher macrophages and proliferating cells compared to SPF datasets, possibly due to the presence of microbial exposure [24] (Figure 5B) (Figure S8D). T cell atlas confirmed a naïve-to-memory imbalance and expansion of eTregs and Tfh cells (Figure 5C,D) (Figure S10). B cell atlas showed robust TrB and FoB reduction with trends in Apoe-hi and memory B cells expansion (Figure 5E,F) (Figure S11). Old NM mice showed strikingly increased memory B cells compared to SPF datasets, indicating the role of continuous microbiota exposure in their generation (Figure 5F) [25].

Cross-dataset DEG analysis revealed conserved signatures in lymphoid but not myeloid/stromal cells (Table S7A). Conserved NK cell ageing signature included loss of cytotoxic genes (*Gzma, Klf2, Prf1, Zeb2*) and gain of other lineage markers (*Ighm, Ly6e*) (Table S7B-C). The pro-inflammatory long non-coding RNA, *AW112010*, was upregulated across multiple T and B cell subsets. T cell subsets displayed conserved stress- and survival-driven transcriptional programmes: naïve T cells lost *Il7r* and *Lef1* while gaining *Socs3* and *Rbm3*; EM T cells gained pro-survival (*Bcl2*), exhaustion (*Lag3*) and inflammatory mediators (*S100a6, Ccl5, Tnfrsf4, Maf, Junb, Nfkbia*), while losing renewal factors (*Lef1, Tcf7*). B cells showed parallel patterns with upregulated stress response and plasma cell differentiation genes (*Rbm3, Cirbp, Psmb8, Psmb9, Ahnak2, Zbtb32, Zbtb20*) and reduced B cell signalling regulators (*Zfp318, Ighd, Cr2, Plac8*). Collectively, these findings highlight conserved ageing signatures of stress adaptation, survival and effector skewing across T and B cells, alongside context-dependent variation shaped by strain, platform and environment.

3 | Discussion

We generated a single-cell transcriptomic atlas of ageing murine splenocytes, providing high-resolution insights into spleen-specific immune heterogeneity. Our cross-cohort atlas uncovered conserved ageing signatures across lymphoid cell types beyond strains, platforms, and experimental contexts.

Ageing imposes convergent transcriptional programs across lymphocyte lineages, fundamentally reorienting immune priorities from pathogen defence towards cellular self-preservation through heightened stress adaptation and regulatory bias. As expected, ageing reduced the naïve pool and expanded EM and activated Treg states, consistent with thymic involution and lifelong antigen exposure [1, 8, 16, 26–28]. Both naïve and EM T cells downregulated quiescence and migration genes while upregulating activation and stress-response genes [29, 30]. Within CD8EM Gzmk+ T cells, Gzmk-hi cells, characterised by self-renewal capacity, showed loss of migratory and infection responses along with a gain of exhaustion/survival capacity, possibly indicating a shift towards tissue-resident Gzmk-lo phenotype with ageing. Conversely, Gzmk-lo cells enriched in aged mice showed pronounced inflammatory signatures, consistent with their role as drivers of inflammageing and tissue pathology [16].

The ageing B cell compartment shifted towards mature and age-associated subsets (memory B, Bregs, Apoe-hi, and ABCs) with reduced differentiation and activation genes, creating a microenvironment that impairs vaccine responses and promotes autoimmunity [31, 32]. Despite increased Tfh frequency, GC B cells declined, consistent with reports that aged Tfh cells exhibit defective function and GC localisation, thereby disrupting T–B collaboration and humoral responses [33, 34]. Together, our findings show that splenic immunosenescence represents active transcriptional reprogramming that prioritises survival over surveillance, an evolutionarily conserved trade-off with implications for healthy ageing interventions.

Chronic stress in old mice showed modest compositional and transcriptomic shifts in splenocytes, revealing that age-associated transcriptional reprogramming dominates the cellular landscape. This supports the view that chronic stress adds nuanced, cell type- and timing-dependent immunomodulation rather than broadly amplifying age-associated phenotypes [35, 36].

By integrating multiple SPF datasets, we identified cross-study ageing signatures (NK cytotoxic erosion, naïve-to-effector phenotype, and memory-skewed B-cell states) from context-dependent variations (strain, platform and microbiota) that are well-recognised modifiers of immune ageing [37]. Higher doublet proportions in NM mice reflect the technology used, as previously reported [38]. The absence of distinct ABCs in the atlas likely reflects technical constraints of cross-platform integration, while Breg absence may stem from microbiota-driven emergence or similar phenotyping limitations [39, 40].

Conserved ageing signatures included reduced NK maturation and cytotoxicity (*Gzma, Klf2, Prf1, Zeb2*), with aberrant *Ighm* expression linked to dysfunctional NK phenotypes in human autoimmune disease [41]. Naive T cells downregulated quiescence (*Lef1, Il7r*) and upregulated inflammation/stress-response genes (*Socs3, Rbm3*) indicating impaired homeostatic maintenance [42, 43]. Similarly, EM T cells showed loss of quiescence (*Lef1, Tcf7*) and gain of inflammatory/exhaustion/survival genes (*S100a6, Ccl5, Tnfrsf4, Maf, Junb, Nfkbia, Lag3, Bcl2*) supporting inflammageing [43]. B cells increased stress/differentiation genes (*Rbm3, Cirbp, Psmb8, Psmb9, Ahnak2, Zbtb32, Zbtb20*) while decreasing signalling regulators (*Zfp318, Ighd, Cr2, Plac8*), consistent with dysfunctional mature B cell expansion [44, 45]. These changes suggest convergent ageing patterns within the adaptive compartment, potentially reducing effective immune responses. The absence of conserved myeloid signatures was likely due to lower cell proportions and their increased environmental sensitivity, amplifying the impact of inter-study technical variations [46].

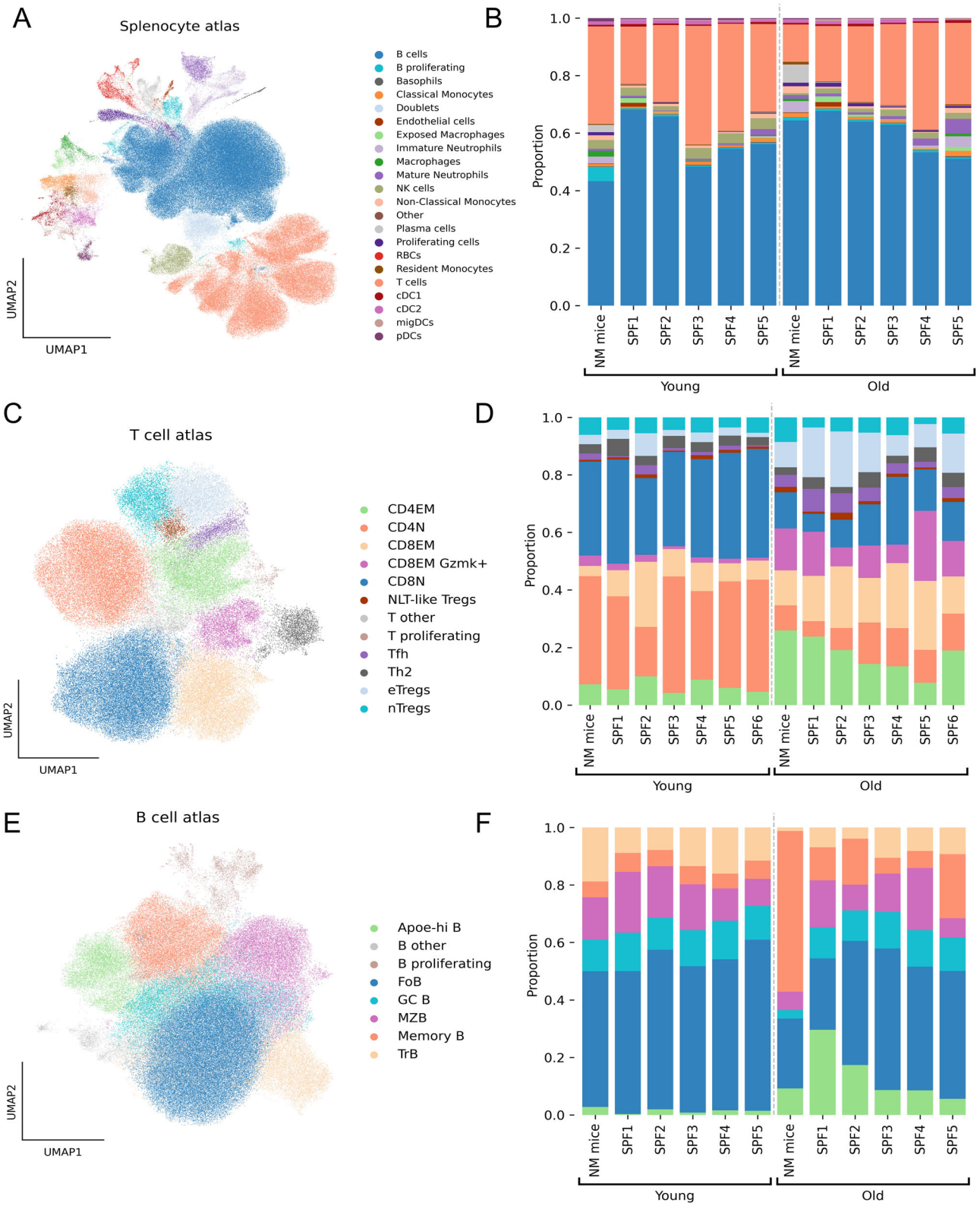

FIGURE 5 | Cross-dataset integration and characterisation of splenocyte diversity. (A) UMAP visualising integrated splenocyte atlas with subsets identified by Leiden clustering and marker gene expression. (B) Relative proportion of splenocytes in young and old mice. Each stacked bar represents one group normalised to 1.0 indicating 100% of cells within a group and each colour represents one cell type. (C) UMAP representation of integrated T cell atlas identified by Leiden clustering and marker gene expression. (D) Relative proportion of T cell subsets in young and old mice. Each stacked bar represents one group normalised to 1.0 indicating 100% of cells within a group and each colour represents one cell type. (E) UMAP of integrated B cell atlas identified by Leiden clustering and marker gene expression. (F) Relative proportion of B cell subsets in young and old mice. Each stacked bar represents one group normalised to 1.0 indicating 100% of cells within a group and each colour represents one cell type.

Collectively, our results demonstrate splenic immune ageing as a coordinated shift from activation and plasticity towards survival, stress adaptation, and effector states across T and B lineages. Our atlas provides a reference for benchmarking interventions, such as vaccination adjuvants, metabolic modulators, and microbiota-targeted therapies, against conserved immunosenescence hallmarks and for dissecting why some ageing phenotypes generalise while others remain context-bound.

3.1 | Data Limitations and Perspectives

Our study has several limitations. First, strain and sequencing platform variability likely contributed to context-dependent differences in cell abundance and gene expression observed between NM mice and other datasets in the spleen atlas. The absence of specific cell subsets (ABCs) may reflect technical constraints of cross-platform integration rather than biological absence, highlighting the need for parallel SPF and NM mice experiments to accurately assess microbiota effects on immune ageing. Second, our chronic stress paradigm uses a single timeframe, potentially underestimating prolonged stress impacts. Third, functional validation of subset-specific vulnerabilities is essential to establish causal links to impaired immunity.

Future directions include incorporating multi-omic modalities, longitudinal sampling, and broader tissue coverage to capture systemic ageing trajectories in NM mice. Disentangling strain, sex, and microbiota contributions will be critical for translating murine insights into human immune ageing.

4 | Methods

4.1 | Animals

Young (4-month-old; $n = 5$) and old (22–24-month-old; $n = 11$) female Balb/c mice were used. This study was approved by the Animal Experiments Ethics Committee at the Ministry of Regional Affairs and Agriculture (Estonia) under Protocol No. 1368. All methods complied with ARRIVE guidelines. Young mice were acquired from the Laboratory Animal Centre, Institute of Biomedicine and Translational Medicine, Tartu. Mice were enriched with NM by weekly addition of fomite bedding from wild mice obtained from Tallinn Zoo. Mice were housed communally with a standard 12 h dark cycle and fed *ad libitum*.

4.2 | CVS Regimen

Old NM mice were subjected to CVS protocol as detailed in Table S1B [47]. Stressed mice ($n = 6$) received random daytime and nighttime stressors over 14 days, while control mice ($n = 5$) were left undisturbed with food and water *ad libitum*. Mice losing > 20% body weight were euthanised by decapitation. Serum corticosterone was measured using enzyme immunoassay kits (Arbor Assays). For experimental termination, mice were euthanised with ketamine and xylazine overdose intraperitoneally.

4.3 | Splenocyte Isolation and Parse scRNA-seq Processing

Harvested spleens were mashed between glass slides and erythrocytes were lysed using red blood lysis buffer. Splenocytes were filtered and counted on LUNA-FL Dual Fluorescence Cell Counter (Logos Biosystems). Samples were fixed using Fixation Kit (Parse Biosciences) and stored at −80°C per manufacturer's protocol. We loaded 19,230 cells/sample totalling 384,600 cells from 20 samples (16 current dataset samples and four unrelated samples to utilise the maximum capacity of the kit). Samples were multiplexed and processed using Parse WT kit targeting 100,000 cell recovery (5000 cells/sample). Nine sub-libraries including one test sub-library were generated and sequenced as paired-end 150-bp reads using Illumina NovaSeq 6000.

4.4 | scRNA-seq Data Pre-Processing and QC

Raw sequencing data were processed using Split-pipe pipeline (Parse Biosciences). An indexed genome was constructed using Ensembl's mm10 mouse genome. Each sub-library was processed individually and then merged to generate a unified gene expression matrix. Combined matrices were imported into Scanpy for pre-processing [48]. QC was performed independently per sample to eliminate low-quality or contaminating cells based on total unique molecular identifiers (UMIs) and mitochondrial gene content. QC thresholds were selected through visual inspection of UMI/cell and mitochondrial gene expression distributions. Similar QC was performed for each publicly available dataset in the atlas.

4.5 | Data Integration and Clustering

scVI was used to integrate samples across NM mice sub-libraries and datasets across the atlas, correcting batch effects and accommodating heterogeneous data sources [49, 50]. For all cells, the top 5000 highly variable genes were selected (3000 for re-clustering T and B cells; 2000 for CD8EM Gzmk+) and merged using Scanpy. The scVI model used raw gene expression counts with dataset and sample identifiers as categorical covariates and mitochondrial gene percentage as continuous covariate. Dimensionality reduction and clustering used Scanpy with Leiden clustering at multiple resolutions. Cluster identities were assigned based on canonical marker expression.

4.6 | DEG Analysis

Pseudobulk DEG analysis was performed on NM mice dataset using DESeq2 (R package) [51]. Cell types with < 2 replicates per group and < 10 counts across samples were excluded. Genes were considered significant at log2 fold change > 0.25 and false discovery rate (FDR) < 0.05 (Benjamini–Hochberg correction). For atlas-level DEG analysis, Wilcoxon rank-sum test (Scanpy) was implemented. Cell types with < 10 cells per group were excluded. Genes were considered significant at log-fold change > 0.25, FDR < 0.05 (Benjamini–Hochberg correction) and expression in > 10% of cells in old group.

4.7 | General Statistics and Plots

For NM mice cell type proportions, Welch's two-sample *t*-test was used. Data represent mean ± SEM. To quantify age-related changes across atlas datasets, we performed random-effects meta-analysis of cell type proportions. For each cell type, log2 fold changes between old and young groups were calculated and merged using inverse-variance weighting with the DerSimonian–Laird method. Heterogeneity was assessed using I^2 statistics. *p*-values were FDR-corrected (Benjamini–Hochberg correction) with FDR < 0.05 considered significant.

Author Contributions

Chinna Susan Philip: conceptualisation, investigation, project administration, data curation, formal analysis, visualisation, writing – original draft, review and editing. **Igor Filippov**: conceptualisation, data curation, formal analysis, visualisation. **Uku Haljasorg**: investigation. **Pärt Peterson**: conceptualisation, supervision, funding acquisition, writing – review and editing. All authors have read and approved the manuscript.

Acknowledgements

This study was supported by the European Union's Horizon 2020 research and innovation programme under the Marie Skłodowska-Curie grant agreement no: 955321, EU Horizon WIDERA 2023 under grant agreement no: 101159920, and Estonian Research Council grants (PRG2011 and TARISTU24-TK22).

Conflicts of Interest

The authors declare no conflicts of interest.

Data Availability Statement

NM mice dataset analysed in this study is available in the Gene Expression Omnibus (GEO) repository under accession number GSE2406. Additional publicly available datasets were obtained from GEO (GSE132901, GSE155006, GSE179095, and GSE210719), the AWS S3 bucket (https://registry.opendata.aws/tabula-muris-senis/), and the Genome Sequence Archive (GSA: CRA004660). All scripts used for data analysis and batch-corrected atlas objects are available from Zenodo at: https://doi.org/10.5281/zenodo.18380353.

4.8 | Peer Review

The peer review history for this article is available at https://publons.com/publon/10.1002/eji.70170.

References

1. The Tabula Muris Consortium, "A Single-Cell Transcriptomic Atlas Characterizes Ageing Tissues in the Mouse," *Nature* 583, no. 7817 (July 2020): 590–595.

2. M. Arif, A. Lehoczki, G. Haskó, F. W. Lohoff, Z. Ungvari, and P. Pacher, "Global and Tissue-Specific Transcriptomic Dysregulation in Human Aging: Pathways and Predictive Biomarkers," *GeroScience* 47, no. 4 (April 2025): 5917–5936, https://doi.org/10.1007/s11357-025-01672-z.

3. V. Budamagunta, T. C. Foster, and D. Zhou, "Cellular Senescence in Lymphoid Organs and Immunosenescence," *Aging* 13, no. 15 (August 2021): 19920–19941, https://doi.org/10.18632/aging.203405.

4. V. Bronte and M. J. Pittet, "The Spleen in Local and Systemic Regulation of Immunity," *Immunity* 39, no. 5 (November 2013): 806–818, https://doi.org/10.1016/j.immuni.2013.10.010.

5. I. den Braber, T. Mugwagwa, N. Vrisekoop, et al., "Maintenance of Peripheral Naive T Cells Is Sustained by Thymus Output in Mice but Not Humans," *Immunity* 36, no. 2 (February 2012): 288–297.

6. A. E. Kmieciak, L. V. Brown, M. C. Coles, J. Wagg, A. Phipps, and E. A. Gaffney, "Predicted Limited Redistribution of T Cells to Secondary Lymphoid Tissue Correlates With Increased Risk of Haematological Malignancies in Asplenic Patients," *Scientific Reports* 11, no. 1 (August 2021): 16394, https://doi.org/10.1038/s41598-021-95225-x.

7. V. M. Turner and N. A. Mabbott, "Influence of Ageing on the Microarchitecture of the Spleen and Lymph Nodes," *Biogerontology* 18, no. 5 (October 2017): 723–738, https://doi.org/10.1007/s10522-017-9707-7.

8. J. C. Kimmel, L. Penland, N. D. Rubinstein, D. G. Hendrickson, D. R. Kelley, and A. Z. Rosenthal, "Murine Single-Cell RNA-seq Reveals Cell-Identity- and Tissue-Specific Trajectories of Aging," *Genome Research* 29, no. 12 (December 2019): 2088–2103, https://doi.org/10.1101/gr.253880.119.

9. B. R. Becklund, J. F. Purton, C. Ramsey, et al., "The Aged Lymphoid Tissue Environment Fails to Support Naïve T Cell Homeostasis," *Scientific Reports* 6, no. 1 (August 2016): 30842, https://doi.org/10.1038/srep30842.

10. V. M. Turner and N. A. Mabbott, "Ageing Adversely Affects the Migration and Function of Marginal Zone B Cells," *Immunology* 151, no. 3 (July 2017): 349–362, https://doi.org/10.1111/imm.12737.

11. M. Verheijen, S. Rane, C. Pearson, A. J. Yates, and B. Seddon, "Fate Mapping Quantifies the Dynamics of B Cell Development and Activation Throughout Life," *Cell Reports* 33, no. 7 (November 2020): 108376, https://doi.org/10.1016/j.celrep.2020.108376.

12. K. B. Menees, R. H. Earls, J. Chung, et al., "Sex- and Age-Dependent Alterations of Splenic Immune Cell Profile and NK Cell Phenotypes and Function in C57BL/6J Mice," *Immunity & Ageing* 18 (January 2021): 3, https://doi.org/10.1186/s12979-021-00214-3.

13. A. G. Groenen, M. Lipscomb, and R. Bossardi Ramos, "Resolvin D1 Suppresses Macrophage Senescence and Splenic Fibrosis in Aged Mice," *Prostaglandins, Leukotrienes, and Essential Fatty Acids* 202 (March 2024): 102634, https://doi.org/10.1016/j.plefa.2024.102634.

14. C. P. Wong, K. R. Magnusson, and E. Ho, "Aging Is Associated With Altered Dendritic Cells Subset Distribution and Impaired Proinflammatory Cytokine Production," *Experimental Gerontology* 45, no. 2 (February 2010): 163–169, https://doi.org/10.1016/j.exger.2009.11.005.

15. A. A. van Beek, F. Fransen, B. Meijer, P. de Vos, E. F. Knol, and H. F. J. Savelkoul, "Aged Mice Display Altered Numbers and Phenotype of Basophils, and Bone Marrow-Derived Basophil Activation, With a Limited Role for Aging-Associated Microbiota," *Immunity & Ageing* 15 (November 2018): 32.

16. D. A. Mogilenko, O. Shpynov, P. S. Andhey, et al., "Comprehensive Profiling of an Aging Immune System Reveals Clonal GZMK+ CD8+ T Cells as Conserved Hallmark of Inflammaging," *Immunity* 54, no. 1 (January 2021): 99–115.e12, https://doi.org/10.1016/j.immuni.2020.11.005.

17. C. E. Lyons, J. P. Pallais, S. McGonigle, et al., "Chronic Social Stress Induces p16-Mediated Senescent Cell Accumulation in Mice," *Nature Aging* 5, no. 1 (January 2025): 48–64, https://doi.org/10.1038/s43587-024-00743-8.

18. C. E. Lyons, M. Razzoli, and A. Bartolomucci, "The Impact of Life Stress on Hallmarks of Aging and Accelerated Senescence: Connections in Sickness and in Health," *Neuroscience and Biobehavioral Reviews* 153 (October 2023): 105359, https://doi.org/10.1016/j.neubiorev.2023.105359.

19. L. Lei, Y. Li, M. Li, et al., "Pathological Changes in the Spleen of Mice Subjected to Different Time Courses of Restraint Stress," *Scientific Reports* 14, no. 1 (June 2024): 13543, https://doi.org/10.1038/s41598-024-64475-w.

20. W. Jiang, Y. Li, J. Sun, et al., "Spleen Contributes to Restraint Stress Induced Changes in Blood Leukocytes Distribution," *Scientific Reports* 7, no. 1 (July 2017): 6501, https://doi.org/10.1038/s41598-017-06956-9.

21. S. Ma, S. Wang, Y. Ye, et al., "Heterochronic Parabiosis Induces Stem Cell Revitalization and Systemic Rejuvenation Across Aged Tissues," *Cell Stem Cell* 29, no. 6 (June 2022): 990–1005.e10, https://doi.org/10.1016/j.stem.2022.04.017.

22. A. B. Schroer, P. B. Ventura, J. Sucharov, et al., "Platelet Factors Attenuate Inflammation and Rescue Cognition in Ageing," *Nature* 620,

no. 7976 (August 2023): 1071–1079, https://doi.org/10.1038/s41586-023-06436-3.

23. D. J. Tyrrell, K. M. Wragg, J. Chen, et al., "Clonally Expanded Memory CD8+ T Cells Accumulate in Atherosclerotic Plaques and Are Pro-Atherogenic in Aged Mice," *Nature Aging* 3, no. 12 (December 2023): 1576–1590, https://doi.org/10.1038/s43587-023-00515-w.

24. S. Abolins, E. C. King, L. Lazarou, et al., "The Comparative Immunology of Wild and Laboratory Mice, *Mus musculus domesticus*," *Nature Communications* 8, no. 1 (May 2017): 14811, https://doi.org/10.1038/ncomms14811.

25. M. Z. Syeda, T. Hong, C. Huang, W. Huang, and Q. Mu, "B Cell Memory: From Generation to Reactivation: A Multipronged Defense Wall Against Pathogens," *Cell Death Discovery* 10, no. 1 (March 2024): 117, https://doi.org/10.1038/s41420-024-01889-5.

26. C. R. Arnold, J. Wolf, S. Brunner, D. Herndler-Brandstetter, and B. Grubeck-Loebenstein, "Gain and Loss of T Cell Subsets in Old Age—Age-Related Reshaping of the T Cell Repertoire," *Journal of Clinical Immunology* 31, no. 2 (April 2011): 137–146, https://doi.org/10.1007/s10875-010-9499-x.

27. G. Oldenhove, N. Bouladoux, and E. A. Wohlfert, "Decrease of Foxp3+ Treg Cell Number and Acquisition of Effector Cell Phenotype During Lethal Infection," *Immunity* 31, no. 5 (November 2009): 772–786, https://doi.org/10.1016/j.immuni.2009.10.001.

28. B. Santner-Nanan, N. Seddiki, E. Zhu, et al., "Accelerated Age-Dependent Transition of Human Regulatory T Cells to Effector Memory Phenotype," *International Immunology* 20, no. 3 (March 2008): 375–383, https://doi.org/10.1093/intimm/dxm151.

29. M. Jia, K. Sayed, M. G. Kapetanaki, et al., "LEF1 Isoforms Regulate Cellular Senescence and Aging," *Aging Cell* 22, no. 12 (2023): e14024, https://doi.org/10.1111/acel.14024.

30. B. González-Bermúdez, H. Kobayashi, A. Abarca-Ortega, et al., "Aging Is Accompanied by T-Cell Stiffening and Reduced Interstitial Migration Through Dysfunctional Nuclear Organization," *Immunology* 167, no. 4 (2022): 622–639, https://doi.org/10.1111/imm.13559.

31. J. Chen, J. C. Deng, and D. R. Goldstein, "How Aging Impacts Vaccine Efficacy: Known Molecular and Cellular Mechanisms and Future Directions," *Trends in Molecular Medicine* 28, no. 12 (December 2022): 1100–1111, https://doi.org/10.1016/j.molmed.2022.09.008.

32. K. M. Nickerson, S. Smita, K. B. Hoehn, et al., "Age-Associated B Cells Are Heterogeneous and Dynamic Drivers of Autoimmunity in Mice," *Journal of Experimental Medicine* 220, no. 5 (May 2023): e20221346, https://doi.org/10.1084/jem.20221346.

33. A. Silva-Cayetano, S. Fra-Bido, P. A. Robert, et al., "Spatial Dysregulation of T Follicular Helper Cells Impairs Vaccine Responses in Aging," *Nature Immunology* 24, no. 7 (July 2023): 1124–1137, https://doi.org/10.1038/s41590-023-01519-9.

34. P. T. Sage, C. L. Tan, G. J. Freeman, M. Haigis, and A. H. Sharpe, "Defective TFH Cell Function and Increased TFR Cells Contribute to Defective Antibody Production in Aging," *Cell Reports* 12, no. 2 (July 2015): 163–171, https://doi.org/10.1016/j.celrep.2015.06.015.

35. F. S. Dhabhar, "Enhancing Versus Suppressive Effects of Stress on Immune Function: Implications for Immunoprotection Versus Immunopathology," *Allergy, Asthma, and Clinical Immunology* 4, no. 1 (March 2008): 2, https://doi.org/10.1186/1710-1492-4-1-2.

36. V. A. Macht and L. P. Reagan, "Chronic Stress From Adolescence to Aging in the Prefrontal Cortex: A Neuroimmune Perspective," *Frontiers in Neuroendocrinology* 49 (April 2018): 31–42, https://doi.org/10.1016/j.yfrne.2017.12.001.

37. J. Nikolich-Žugich, "The Twilight of Immunity: Emerging Concepts in Aging of the Immune System," *Nature Immunology* 19, no. 1 (January 2018): 10–19, https://doi.org/10.1038/s41590-017-0006-x.

38. I. Filippov, C. S. Philip, L. Schauser, and P. Peterson, "Comparative Transcriptomic Analyses of Thymocytes Using 10x Genomics and Parse scRNA-seq Technologies," *BMC Genomics* 25, no. 1 (November 2024): 1069, https://doi.org/10.1186/s12864-024-10976-x.

39. J. K. Maerz, C. Trostel, A. Lange, et al., "Bacterial Immunogenicity Is Critical for the Induction of Regulatory B Cells in Suppressing Inflammatory Immune Responses," *Frontiers in Immunology* 10 (January 2020): 3093.

40. N. Johansen and G. Quon, "scAlign: A Tool for Alignment, Integration, and Rare Cell Identification From scRNA-seq Data," *Genome Biology* 20, no. 1 (August 2019): 166, https://doi.org/10.1186/s13059-019-1766-4.

41. Q. Wang, Q. Li, R. Wang, et al., "Identification of CD8+ T Cell-Related Biomarkers and Immune Infiltration Characteristic of Rheumatoid Arthritis," *Aging* 16, no. 2 (January 2024): 1399–1413, https://doi.org/10.18632/aging.205435.

42. J. Taylor, L. Reynolds, L. Hou, et al., "Transcriptomic Profiles of Aging in Naïve and Memory CD4+ Cells From Mice," *Immunity Ageing* 14, no. 1 (June 2017): 15, https://doi.org/10.1186/s12979-017-0092-5.

43. X. Yang, X. Wang, L. Lei, et al., "Age-Related Gene Alteration in Naïve and Memory T Cells Using Precise Age-Tracking Model," *Frontiers in Cell and Developmental Biology* 8 (February 2021): 624380, https://doi.org/10.3389/fcell.2020.624380.

44. M. Bulati, C. Caruso, and G. Colonna-Romano, "From Lymphopoiesis to Plasma Cells Differentiation, the Age-Related Modifications of B Cell Compartment Are Influenced by "Inflamm-Ageing"," *Ageing Research Reviews* 36 (July 2017): 125–136, https://doi.org/10.1016/j.arr.2017.04.001.

45. Y. Deng, X. He, J. Peng, et al., "Comprehensive Characterisation of Age-Related Changes in Cell Subpopulations and Tissue Structural Properties in Secondary Lymphoid Organs," *Cell Death & Disease* 16, no. 1 (October 2025): 679, https://doi.org/10.1038/s41419-025-08007-y.

46. D. Gosselin, V. M. Link, C. E. Romanoski, et al., "Environment Drives Selection and Function of Enhancers Controlling Tissue-Specific Macrophage Identities," *Cell* 159, no. 6 (December 2014): 1327–1340, https://doi.org/10.1016/j.cell.2014.11.023.

47. J. X. Ding, P. T. Rudak, W. Inoue, and S. M. M. Haeryfar, "Physical Restraint Mouse Models to Assess Immune Responses Under Stress With or Without Habituation," *STAR Protocols* 2, no. 4 (September 2021): 100838, https://doi.org/10.1016/j.xpro.2021.100838.

48. F. A. Wolf, P. Angerer, and F. J. Theis, "SCANPY: Large-Scale Single-Cell Gene Expression Data Analysis," *Genome Biology* 19, no. 1 (February 2018): 15, https://doi.org/10.1186/s13059-017-1382-0.

49. M. D. Luecken, M. Büttner, K. Chaichoompu, et al., "Benchmarking Atlas-Level Data Integration in Single-Cell Genomics," *Nature Methods* 19, no. 1 (January 2022): 41–50, https://doi.org/10.1038/s41592-021-01336-8.

50. R. Lopez, J. Regier, M. B. Cole, M. I. Jordan, and N. Yosef, "Deep Generative Modeling for Single-Cell Transcriptomics," *Nature Methods* 15, no. 12 (December 2018): 1053–1058, https://doi.org/10.1038/s41592-018-0229-2.

51. M. I. Love, W. Huber, and S. Anders, "Moderated Estimation of Fold Change and Dispersion for RNA-seq Data With DESeq2," *Genome Biology* 15, no. 12 (2014): 550, https://doi.org/10.1186/s13059-014-0550-8.

Supporting Information

Additional supporting information can be found online in the Supporting Information section.

Supporting File 1: eji70170-sup-0001-SupMat.docx.
Supporting File 2: eji70170-sup-0002-TableS1.xlsx.
Supporting File 3: eji70170-sup-0003-TableS2.xlsx.
Supporting File 4: eji70170-sup-0004-TableS3.xlsx.
Supporting File 5: eji70170-sup-0005-TableS4.xlsx.
Supporting File 6: eji70170-sup-0006-TableS5.xlsx.
Supporting File 7: eji70170-sup-0007-TableS6.xlsx.
Supporting File 8: eji70170-sup-0008-TableS7.xlsx.